# Electronic Supplementary Information (ESI)

**Unusual formation of hollow $NiCoO_2$ sub-microspheres by oxygen functional groups dominated thermally induced mass relocation towards efficient lithium storage**

Zhengluo Wang,[a, b] Dienguila Kionga Denis,[a] Zhiwei Zhao,[b] Xuan Sun,[a] Jinyang Zhang,[a] Linrui Hou,[a] Changzhou Yuan [a, b]*

[a] *School of Materials Science & Engineering, University of Jinan, Jinan, 250022, P. R. China*

Email: mse_yuancz@ujn.edu.cn; ayuancz@163.com

[b] *School of Materials Science & Engineering, Anhui University of Technology, Ma'anshan, 243002, P. R. China*

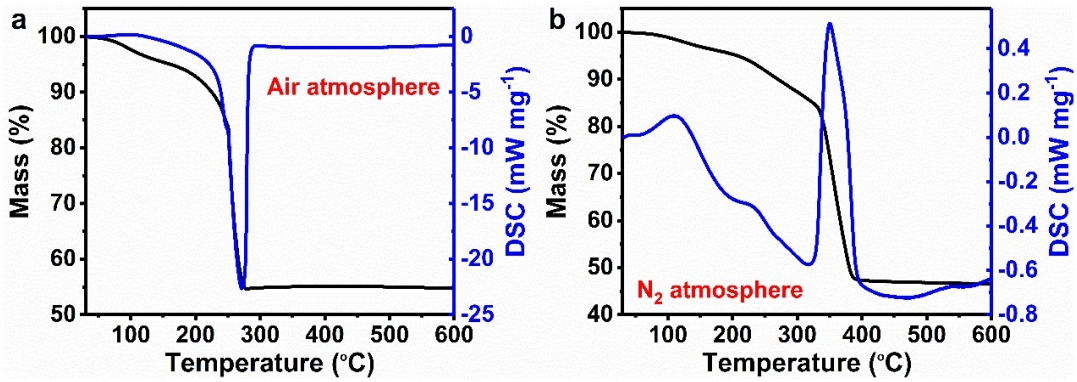


**Fig. S1** TG-DSC plots of (a) the NCGS in air, and (b) the pretreated product in $N_2$ with a temperature ramp of 10 ℃ $min^{-1}$.

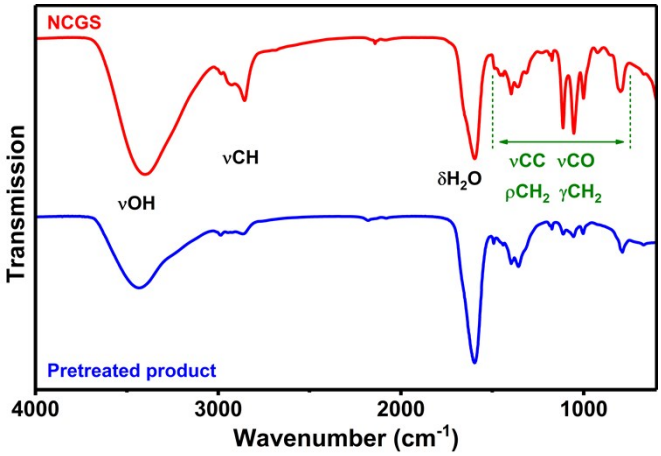


**Fig. S2** FT-IR spectra for the NCGS and pretreated product as indicated.

As shown in **Figure S2**, the strong absorption bands in the 2500 – 3000 $cm^{-1}$ are characteristic of the C-H stretching mode. The wide hump centered at 3400 $cm^{-1}$ and the sharp hump at 1600 $cm^{-1}$ are attributed to the $\nu$(O-H) and $\delta(H_2O)$. All the bands below 1500 $cm^{-1}$ are attributed to the $\nu$(C-C), $\nu$(C-O), $\rho(CH_2)$, $\gamma(CH_2)$ and metal-oxygen (M-O). After pretreated in air, the signals of other bands including $\delta(H_2O)$, $\nu$(O-H), $\nu$(C-H), $\nu$(C-C), $\nu$(C-O), $\rho(CH_2)$ and $\gamma(CH_2)$, are weakened, which demonstrates the evaporation of absorbed water and oxidative decomposition of the organic moiety. Specifically, this characteristic M-O signal almost disappears in the pretreated product, indicating the pretreatment consumes a large amount of oxygen-enriched organic groups.

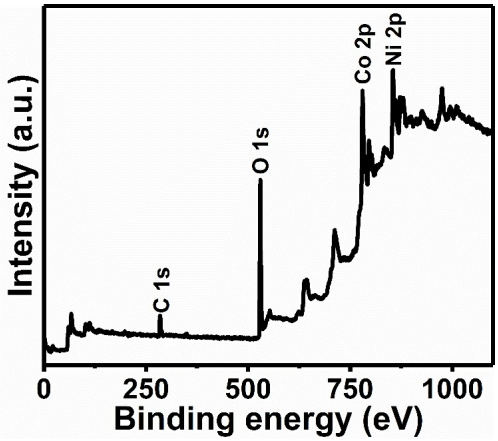


**Fig. S3** XPS full spectrum of the NCOHS.

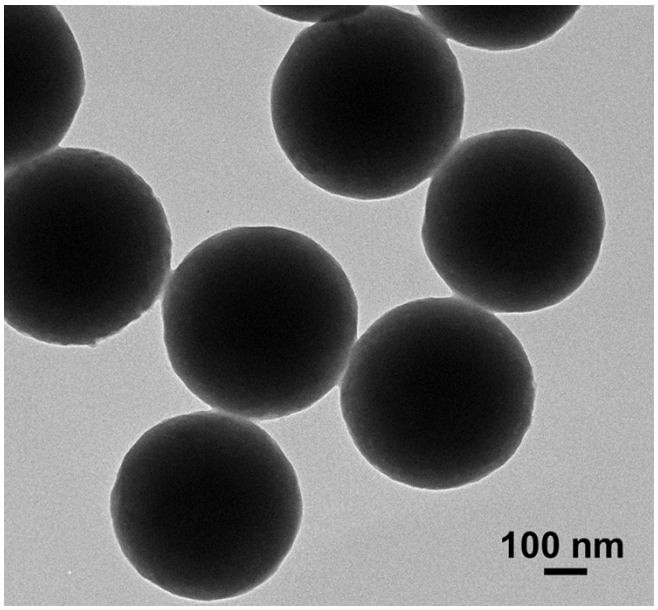


**Fig. S4** TEM image of pretreated product.

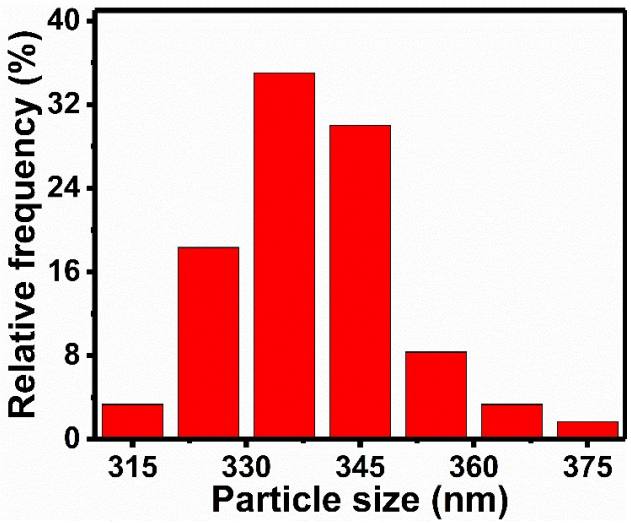


**Fig. S5** Corresponding particle size distribution diagram for the NCOHS.

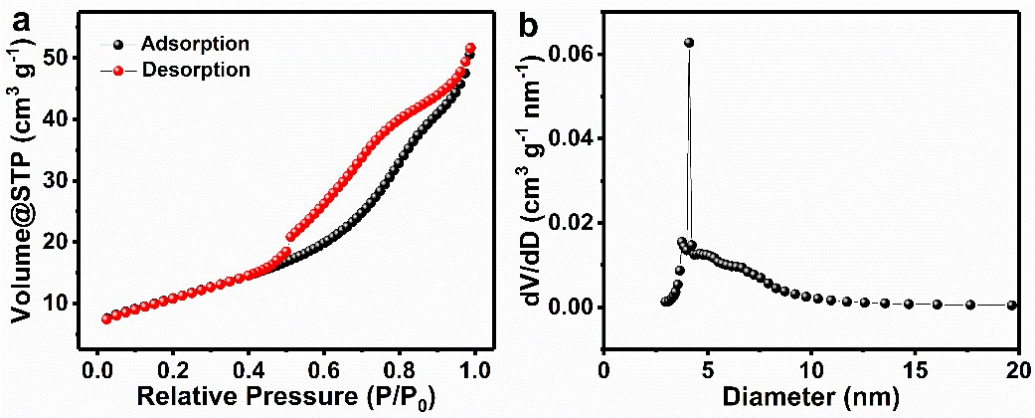


**Fig. S6** (a) $N_2$ sorption isotherms and (b) pore size distribution plot of the NCOHS.

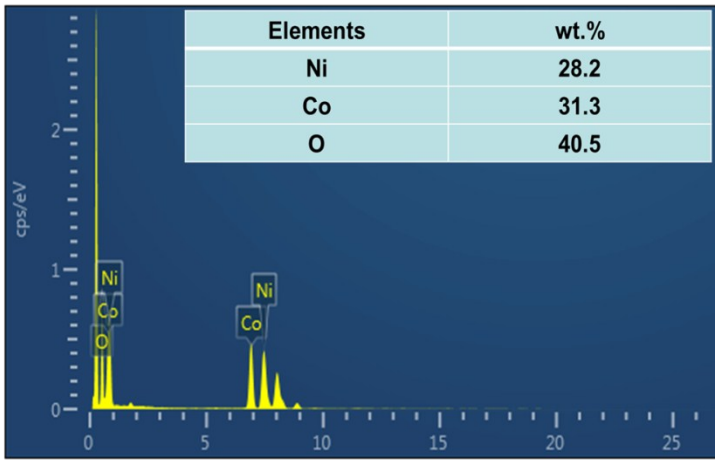


**Fig. S7** EDX spectrum and corresponding elemental ratio (the inset) of the NCOHS.

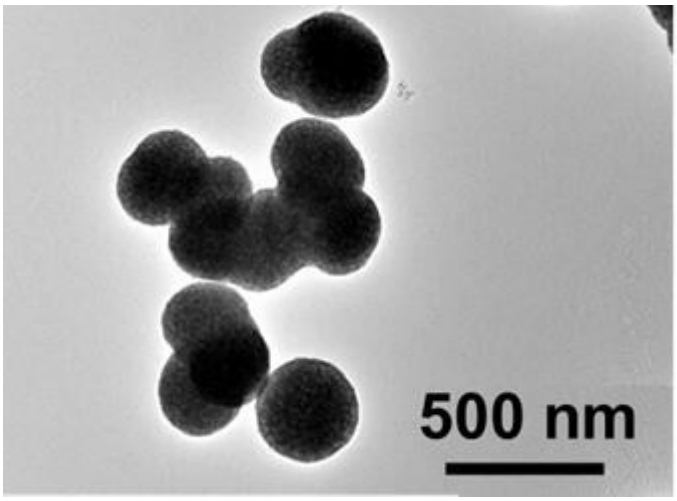


**Fig. S8** TEM image of the product obtained with the absence of the pretreatment in air.

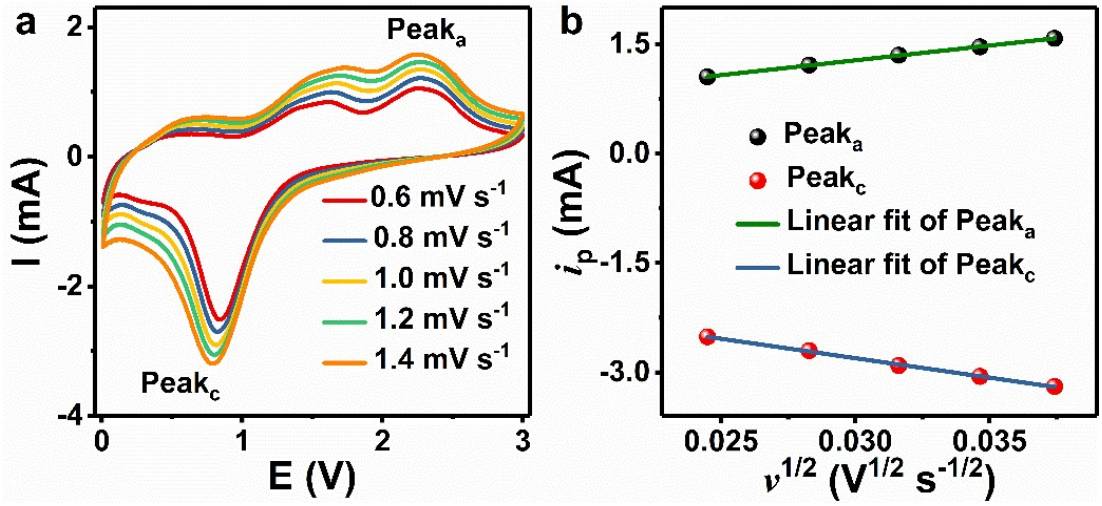


**Fig. S9** (a) CV curves at various scan rates, and (b) the relationship of the peak current ($i_p$) of the $Peak_a$ and $Peak_c$ and the square root of scan rate ($v^{1/2}$) of the NCOHS.

The chemical diffusion coefficient ($D$) describes the transport property of mobile species, especially for diffusion of lithium in the lattice of the host electrode. The D value, indicative of intrinsic kinetic property of one electrode, can be calculated from the CV curves by using the Randles-Sevcik equation as follows:

$$i_p = 2.69\times10^5 n^{3/2} A D^{1/2} v^{1/2} \Delta C_0$$

where $i_p$ is the peak current, $n$ is the number of electrons per reaction species, $A$ is the contact area between NCOHS and electrolyte (here the geometric area of electrode, 1.13 cm$^2$, is used for simplicity), $D$ is $Li^+$ diffusion coefficient, $v$ is the scan rate, $\Delta C_0$ is the change in $Li^+$ concentration during reaction. As derived from the CV curves of NCOHS (**Figure S9a**), the anodic peaks slightly shift to high potential and the cathodic peaks slightly shift to low potential with increasing scan rate. The peak $i_p$ values of both $Peak_a$ and $Peak_c$ exhibit a linear relation with the $v^{1/2}$ (**Figure S9b**). The $Li^+$ diffusion coefficient are estimated as high as $3.66\times10^{-8}$ cm$^2$ s$^{-1}$ and $6.32\times10^{-8}$ cm$^2$ s$^{-1}$ for the delithiation and lithiation process, respectively, which should benefit from the unique porous hollow nanostructure of the NCOHS.

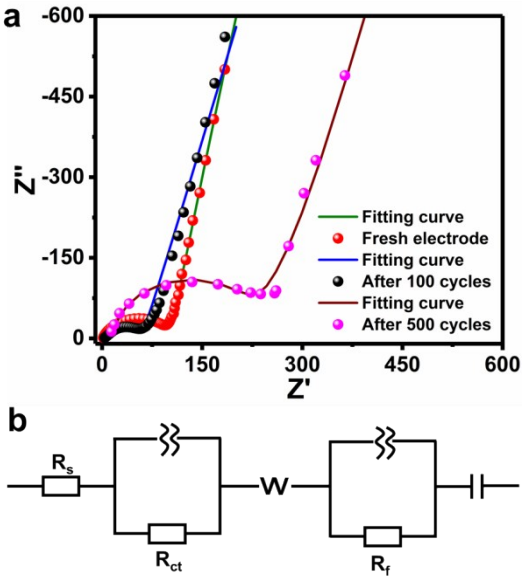


**Fig. S10** (a) Nyquist profiles and fitted plots of the NCOHS electrode at a fully charged state before, and after 100 and 500 cycles, and (b) corresponding equivalent circuit applied for fitting the EIS plots

**Table S1.** Comparisons in electrochemical performance of various Ni-Co-mixed metal oxides with the NCOHS electrode

| Active materials | Initial CE (%) | Specific capacity (mAh $g^{-1}$) | Reference |
|---|---|---|---|
| Single-crystal mesoporous $CoNiO_2$ microflower | 65.6<br>0.1 A $g^{-1}$ | ~397.4<br>110 cycles, 100 mA $g^{-1}$ | **1**<br>Electrochim. Acta |
| Mesoporous $CoNiO_2$ hierarchical structures | 65.6<br>0.1 A $g^{-1}$ | ~449.3<br>50 cycles, 100 mA $g^{-1}$ | **2**<br>New J. Chem. |
| Spherical $NiCoO_2$ nanosheets@C | < 70<br>0.4 A $g^{-1}$ | ~574<br>200 cycles, 400 mA $g^{-1}$ | **3**<br>Nano Energy |
| $NiCoO_2$ nanosheets nanotubes | < 70<br>0.2 A $g^{-1}$ | < 300<br>100 cycles, 200 mA $g^{-1}$ | **4**<br>J. Mater. Chem. A |
| $NiCoO_2$/Carbon xerogel hybrids | 45.6<br>0.1 A $g^{-1}$ | ~456<br>100 cycles, 100 mA $g^{-1}$ | **5**<br>Electrochim. Acta |
| $NiCoO_2$/Carbon nanofibers | 54.4<br>0.1 A $g^{-1}$ | ~551.8<br>500 cycles, 500 mA $g^{-1}$ | **6**<br>Chem-Eur. J |
| $NiCo_2O_4$ hollow spheres | 66<br>0.15 A $g^{-1}$ | ~706<br>100 cycles, 200 mA $g^{-1}$ | **7**<br>Angew. Chem. Int. Ed. |
| Hierarchical porous flower-like $NiCo_2O_4$ | 70<br>0.1 A $g^{-1}$ | ~640<br>60 cycles, 500 mA $g^{-1}$ | **8**<br>J. Mater. Chem. A |
| Au nanoparticles @$NiCo_2O_4$ nanotubes | < 70<br>0.1 A $g^{-1}$ | ~732.5<br>200 cycles, 100 mA $g^{-1}$ | **9**<br>Nano Energy |
| $NiCo_2O_4$ microrod | < 70<br>0.1 A $g^{-1}$ | ~719<br>600 cycles, 500 mA $g^{-1}$ | **10**<br>ACS Appl. Mater. Interfaces |
| $NiCo_2O_4$/Carbon textiles | 76%<br>0.2 A $g^{-1}$ | ~854<br>100 cycles, 500 mA $g^{-1}$ | **11**<br>Adv. Funct. Mater. |
| $NiCo_2O_4$-rGO | 72.9%<br>0.1 A $g^{-1}$ | ~523<br>100 cycles, 200 mA $g^{-1}$ | **12**<br>J. Mater. Chem. A |
| Ultralight nickel foam@ $NiCo_2O_4$ | /<br>0.5 A $g^{-1}$ | ~459<br>150 cycles, 500 mA $g^{-1}$ | **13**<br>J. Mater. Chem. A |
| $NiCo_2O_4$/graphene nanosheet arrays | /<br>0.1 A $g^{-1}$ | ~806<br>55 cycles, 500 mA $g^{-1}$ | **14**<br>Nano Energy |
| $NiCo_2O_4$ nanosheet | /<br>0.2 A $g^{-1}$ | ~804.8<br>100 cycles, 200 mA $g^{-1}$ | **15**<br>Electrochim. Acta |

| | | | |
|---|---|---|---|
| $NiCo_2O_4$ microflowers | / | ~720 | **16** |
| | 0.1 A $g^{-1}$ | 100 cycles, 500 mA $g^{-1}$ | Electrochim. Acta |
| rGO/ $NiCo_2O_4$ | 61% | ~656.5 | **17** |
| | 0.2 A $g^{-1}$ | 50 cycles, 500 mA $g^{-1}$ | Adv. Energy Mater. |
| Ni-Co-mixed oxide | 69.1% | / | **18** |
| nanoprisms | 0.2 A $g^{-1}$ | / | Adv. Energy Mater. |
| $Ni_xCo_{3-x}O_4$ hollow | 70% | / | **19** |
| microspheres | 0.1 A $g^{-1}$ | / | Small |
| $Ni_xCo_{3-x}O_4$ nanorods | 68.4% | / | **20** |
| | 0.1 A $g^{-1}$ | / | Adv. Funct. Mater. |
| Porous $Ni_xCo_{3-x}O_4$ | 54% | / | **21** |
| nanosheets | 0.1 A $g^{-1}$ | / | ACS Appl. Mater. Interfaces |
| $NiCoO_2$ hollow spheres | 70.5% | ~805.9 | **Our work** |
| | 0.2 A $g^{-1}$ | 750 cycles, 500 mA $g^{-1}$ | |

**References:**


[1] Y. G. Liu, Y. Y. Zhao, Y. L. Yu, M. Ahmad and H. Y. Sun, *Electrochim. Acta*, 2014, **132**, 404.

[2] Y. G. Liu, Y. Y. Zhao, Y. L. Yu, J. P. Li, M. Ahmad and H. Y. Sun, *New J. Chem.*, 2014, **38**, 3084.

[3] J. Liang, K. Xi, G. Q. Tan, S. Chen, T. Zhao, P. R. Coxon, H. -K. Kim, S. J. Ding, Y. Yang, R. V. Kumar and J. Lu, *Nano Energy*, 2016, **27**, 457.

[4] X. Xu, B. T. Dong, S. J. Ding, C. H. Xiao and D. M. Yu, *J. Mater. Chem. A*, 2014, **2**, 13069.

[5] Z. W. Zhang, Q. Li, Z. Q. Li, J. Y. Ma, C. X. Li, L. W. Yin and X. P. Gao, *Electrochim. Acta,* 2016, **203**, 117.

[6] Z. L. Wang, Z. W. Zhao, Y. R. Zhang, X. P. Yang, X. Sun, J. Y. Zhang, L. R. Hou and C. Z. Yuan, *Chem. Eur. J.,* 2019, **25**, 863.

[7] L. F. Shen , L. Yu, X. Y. Yu, X. G. Zhang and X. W. Lou, *Angew. Chem. Int. Ed.*, 2015, **54**, 1868.

[8] L. L. Li, Y. L. Cheah, Y. W. Ko, P. F. Teh, G. Wee , C. L. Wong, S. J. Peng and M. Srinivasan,

*J. Mater. Chem. A*, 2013, **1**, 10935.

[9] J. Zhu, Z. Xu and B. A. Lu, *Nano Energy*, 2014, **7**, 114.

[10] F. Fu, J. D. Li, Y. Z. Yao, X. P. Qin, Y. B. Dou, H. Y. Wang, J. K. Tsui, K. -Y. Chan and M. H. Shao, *ACS Appl. Mater. Interfaces,* 2017, **9**, 16194.

[11] L. F. Shen, Q. Che, H. S. Li and X. G. Zhang, *Adv. Funct. Mater.*, 2014, **24**, 2630.

[12] Y. J. Chen, M. Zhuo, J. W. Deng, Z. Xu, Q. H. Li and T. H. Wang, *J. Mater. Chem.* A, 2014, **2**, 4449.

[13] J. Pu, Z. Q. Liu, Z. H. Ma, J. Wang, L. Zhang, S. Z. Chang, W. L. Wu, Z. H. Shen and H. G. Zhang, *J. Mater. Chem. A*, 2016, **4**, 17394.

[14] Y. J. Chen, J. Zhu, B. H. Qu, B. G. Lu and Z. Xu, *Nano Energy*, 2014, **3**, 88.

[15] Y. Q. Zhu and C. B. Cao, *Electrochim. Acta*, 2015, **176**, 141.

[16] J. M. Xu, L. He, W. Xu, H. B. Tang, H. Liu, T. Han, C. J. Zhang and Y. H. Zhang, *Electrochim. Acta*, 2014, **145**, 185.

[17] G. X. Gao, H. B. Wu and X. W. Lou, *Adv. Energy Mater.*, 2014, **6**, 1400422.

[18] L. Yu, B. Y. Guan, W. Xiao and X. W. Lou, *Adv. Energy Mater.*, 2015, **5**, 1500981.

[19] L. L. Wu, Z. Wang, Y. Long, J. Li, Y. Liu, Q. S. Wang, X. Wang, S. Y. Song, X. G. Liu and H. J. Zhang, *Small*, 2017, **9**, 1604270.

[20] H. Li, M. Liang, W. W. Sun and Y. Wang, *Adv. Funct. Mater.*, 2016, **26**, 1098.

[21] F. C. Zheng, D. Q. Zhu and Q. W. Chen, *ACS Appl. Mater. Interfaces,* 2014, **6**, 9256.

**Table S2**. EIS Fitting data of the NCOHS electrode

| | Fresh electrode (Ohm) | After 100 cycles (Ohm) | After 500 cycles (Ohm) |
|---|---|---|---|
| $R_s$ | 1.3 | 3.9 | 13.8 |
| $R_{ct}$ | 98.6 | 76.8 | 258.6 |